Electronic Supplementary Information for:

Photophysics and Photochemistry of Thermally Activated Delayed Fluorescence Emitters Based on Multiple Resonance Effect: Transient Optical and Electron Paramagnetic Resonance Studies

Xi Chen,[a,§] Lei Sun,[b,§] Andrey A. Sukhanov,[c,§] Sandra Doria,[d,e,§] Laura Bussotti,[d] Jianzhang Zhao,*[a] Haijun Xu,*[b] Bernhard Dick,*[f] Violeta K. Voronkova*[c] and Mariangela Di Donato*[d,e]

[a] State Key Laboratory of Fine Chemicals, Frontier Science Center for Smart Materials, School of Chemical Engineering, Dalian University of Technology, Dalian 116024, P. R. China. *E-mail: zhaojzh@dlut.edu.cn

[b] Jiangsu Co-innovation Center of Efficient Processing and Utilization of Forest Resources, Key Laboratory of Forestry Genetics & Biotechnology of Ministry of Education, Jiangsu Provincial Key Lab for the Chemistry and Utilization of Agro-forest Biomass, College of Chemical Engineering, Nanjing Forestry University, Nanjing, 210037, P. R. China; School of Chemistry and Chemical Engineering, Henan Normal University, Xinxiang, 453002, China. *E-mail: xuhaijun@njfu.edu.cn

[c] Zavoisky Physical-Technical Institute, FRC Kazan Scientific Center of RAS, Kazan 420029, Russia. *Email: vio@kfti.knc.ru

[d] LENS (European Laboratory for Non-Linear Spectroscopy), Via N. Carrara 1, 50019 Sesto Fiorentino (FI), Italy. *Email: didonato@lens.unifi.it

[e] ICCOM-CNR, via Madonna del Piano 10-12, 50019, Sesto Fiorentino (FI), Italy

[f] Lehrstuhl für Physikalische Chemie, Institut für Physikalische und Theoretische Chemie, Universität Regensburg, Regensburg 93053, Germany. *E-mail: Bernhard.Dick@chemie.uni-regensburg.de

§ These authors contributed equally to this work.

Contents

1. General Method and Synthesis

All the chemicals used in synthesis are analytically pure and were used as received, without further purification. UV–vis absorption spectra were measured on a UV-2550 spectrophotometer (Shimadzu Ltd., Japan). Fluorescence emission spectra were recorded with a FS5 spectrofluorometer (Edinburgh instruments Ltd., U.K.). Fluorescence quantum yields (Φ_F) were measured by absolute photoluminescence quantum yield spectrometer (Quantaurus-QY Plus C13534-11, Hamamatsu Ltd., Japan). Luminescence lifetimes of compounds were recorded with an OB920 luminescence lifetime spectrometer (Edinburgh Instruments Ltd., U.K.). The compounds **DABNA-1** and **DtBuCzB** were prepared according to the literature methods.[1, 2] The 1,3-Bis(2,4,6-trimethylphenyl)-1,3-dihydro-2H-imidazol-2-ylidene is commercially available (Energy Chemical Company, CAS: 141556-42-5).

1.1. Femtosecond Transient Absorption Spectroscopy. Femtosecond transient absorption spectra (fs-TA) were acquired on a system based on a Ti: sapphire regenerative amplifier (Coherent Legend Elite) pumped by a Ti: sapphire oscillator (Coherent Micra). The system produces 40 fs pulses at 800 nm, with a repetition rate of 1 kHz and an average power of 3.2 W. Excitation pulses at 400 nm were produced by second harmonic generation of the fundamental laser radiation using a 2 mm thick BBO crystal. Excitation pulses in the UV region at 340/-370 nm were produced by third harmonic generation of the signal output of a commercial optical parametric amplifier (TOPAS, Light Conversion) using two BBO crystals in series. The probe beam has been obtained by focusing a small portion of the fundamental 800 nm beam on a 3 mm CaF_2 crystal, kept under continuous movement to avoid damage. The pump-probe delay has been introduced by sending the portion of the fundamental beam used for white light generation through a motorized translator. After focusing and overlapping the pump and probe beams at the sample position, the probe beam has been directed

through a spectrograph and to the detector. The sample was contained in a 2 mm quartz cuvette mounted on a movable stage, to avoid photodegradation. The data were analysed with a global analysis procedure using the software Glotaran-1.5.1.[3] The number of kinetic components to be used for Global analysis has been estimated by performing a preliminary singular values decomposition (SVD) analysis.

1.2. Nanosecond Transient Absorption Spectroscopy. The ns-TA spectra were acquired on a LP980-K laser flash photolysis spectrometer (Edinburgh Instruments, UK). Before the measurements, the samples were purged with N_2 for 10 minutes and then excited with a nanosecond pulsed laser (Surelite OPO Plus SL I-10, Continuum Ltd., USA). The transient signals were digitized with a Tektronix TDS 3012B oscilloscope and the data were processed with the L900 software.

1.3. Time-Resolved Electron Paramagnetic Resonance Spectroscopy. Samples were dissolved in mixed toluene/2-MeTHF solvent (3:1, v/v). The O_2 in the solvent was removed by five freeze–pump–thaw cycles. The time-resolved continuous-wave (TR CW) EPR measurements were performed on an X-band EPR Elexsys E-580 spectrometer (Bruker) at 80 K with the dielectric ring ER 4118X-MD5-W1 resonator. The signal coming from the detector (diode) is digitized by a SpecJet ultra-fast transient signal averager. The bandwidth of the video amplifier is 20 MHz. Samples were photoexcited by the pulse laser YAG:Nd^{3+} Brillian B (Quantel) laser at 355 nm with energy 5 mJ per pulse at a frequency of 10 Hz. The spectra were simulated using the EasySpin package based on the Matlab.[4]

1.4. Computation Details. The geometries of the lowest triplet state were optimized with the unrestricted DFT method, the B3LYP functional, and the 6-31G(d) basis set,[1] using the Gaussian 16 programs .[5] The calculations involving spin-orbit coupling and wavefunction based methods (ROHF = restricted open shell Hartree Fock, CIS = configuration interaction singles, CASSCF = complete active space self consistent field, NEVPT2 = N-Electron Valence State Perturbation Theory) were performed

with the ORCA programs[6, 7] employing the def2-SVP basis and in some cases also the def2-TZVP basis. The Zero Field Splitting (ZFS) parameters *D* and *E* for the T_1 state were computed from UB3LYP/def2-SVP geometry optimizations as well as ROHF/def2-TZVP calculations at these optimized geometries. In contrast to ROHF, UB3LYP suffers from spin contamination (<S**2> ca. 2.015).

1.5. Synthesis Details.

Compounds **DABNA-1** and **DtBuCzB** were synthesized following the reported method.[2,3]

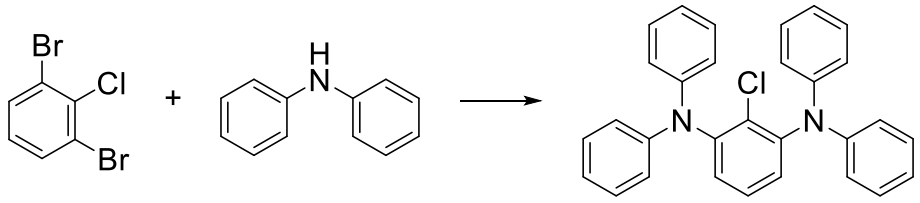

Cl-DABNA-1

Synthesis of Cl-DABNA-1. Under N_2 atmosphere, Diphenylamine (1.69 g, 10 mmol), sodium tert-butoxide (960 mg, 10 mmol), dichlorobis[di-*tert*-butyl (p-dimethylaminophenyl)phosphino]-palladium(II) (354 mg, 0.5 mmol) and 1,3-Dibromo-2-chlorobenzene (1.35 g, 5 mmol) were dissolved in o-xylene (50 mL) and the mixture was stirred at 80 °C for 24 h. After the reaction was finished, the mixture was cooled to room temperature and ethyl acetate and water were added to form a precipitate. The white powder solid was filtered out and dried in vacuum first, then it was further purified by column chromatography with a mixture eluent of dichloromethane/petroleum ether (1:3). After the solvent was removed in vacuo, the crude product was washed with heptane to obtain a white solid (715 mg, yield: 32%).

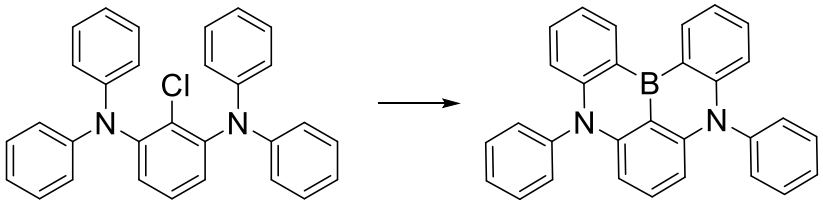

Cl-DABNA-1 **DABNA-1**

Synthesis of DABNA-1. A solution of tert-butyllithium in pentane (3.16 mL, 1.70 M, 5.37 mmol) was added slowly to a solution of **Cl-DABNA-1** (2.0 g, 4.47 mmol) in tert-butylbenzene (25 mL) at –78 ºC under a nitrogen atmosphere. After stirring at –78 ºC for 0.5 h, the reaction mixture was stirred at room temperature for 3 h. After addition of boron tribromide (0.5 mL, 5.39 mmol) at –78 ºC, the reaction mixture was stirred at room temperature for 3 h. *N,N*-Diisopropylethylamine (1.6 mL, 9.11 mmol) was added at 0 ºC and then the reaction mixture was allowed to warm to room temperature. After stirring at 120 ºC for 3 h, the reaction mixture was cooled to room temperature. An aqueous solution of sodium acetate and ethyl acetate was added to the reaction mixture. The aqueous layer was separated and extracted with ethyl acetate. The combined organic layer was condensed in vacuo. it was further purified by column chromatography with using an eluent of petroleum ether. After the solvent was removed in vacuo, the crude product was washed with petroleum ether to obtain a yellow solid (94 mg, yield: 5%). ^{1}H NMR (600 MHz, DMSO-d_6) δ/ppm: 8.883–8.874(d, *J* = 5.68 Hz, 2H),7.801(s, 4H), 7.690(s, 2H), 7.510(s, 2H), 7.439–7.429(d, *J* = 6.19 Hz, 4H), 7.345–7.298(m, 3H), 6.694–6.681(d, *J* = 7.82 Hz, 2H), 6.049–6.037(d, *J* = 7.35 Hz, 2H). MALDI-TOF HRMS($C_{30}H_{21}BN_2^+$) m/z. calcd: 420.1792; found: 420.1779.

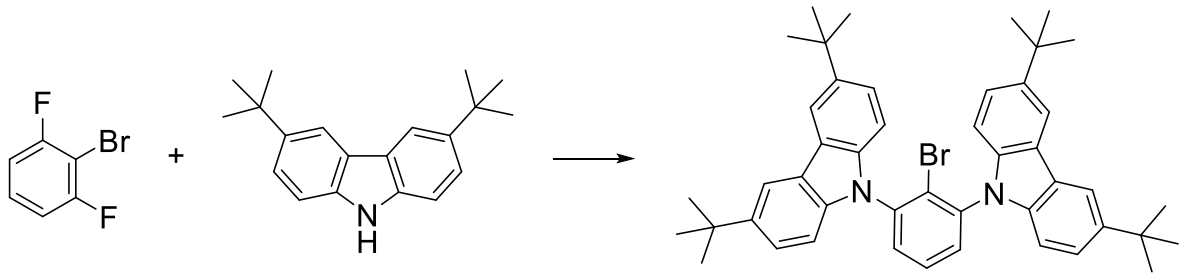

Br-DtBuCzB

Synthesis of Br-DtBuCzB. 10 ml solution of anhydrous DMF (*N,N*-dimethylformamide) which contains 3,6-di-*tert*-butyl-9*H*-carbazole (500 mg, 1.79 mmol)was slowly added dropwise into a mixture of *t*-BuOK (251 mg, 2.24 mmol) and 10 mL anhydrous DMF in a period of 15 min. After the mixture was stirring for 2 h at room temperature, 10 mL anhydrous DMF solution containing 2-bromo-1,3-difluorobenzene (159 mg, 0.82 mmol) was injected dropwise into it within 15 min. The solution was stirred at 140°C for 24 h and then cooled down to room temperature. The resulted solution was poured into ice water (2000 mL). The white powder solid was filtered out and dried in

vacuum first, then it was further purified by column chromatography using a mixture eluent of dichloromethane/petroleum ether (1:4) to obtain a white solid (438 mg, yield: 75%).

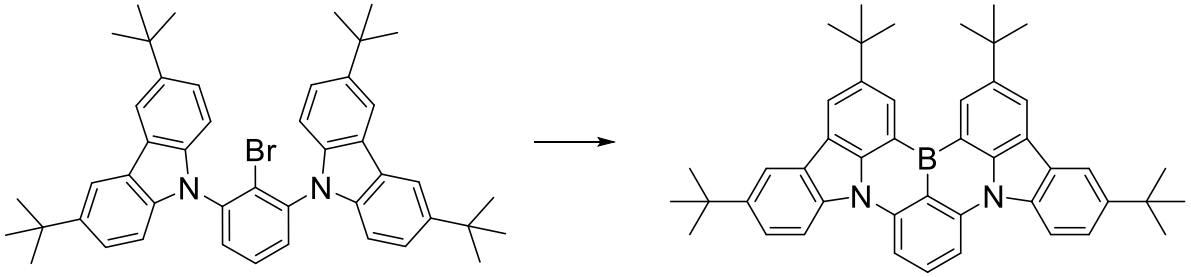

Br-DtBuCzB **DtBuCzB**

Synthesis of DtBuCzB. A solution of *tert*-butyllithium in *n*-hexane (3.2 mL, 1.70 M, 5.37 mmol) was added slowly to a solution of compound **Br-DtBuCzB** (3.18 g, 4.47 mmol) in *tert*-butylbenzene (50 mL) at –78 ºC under a nitrogen atmosphere. After stirring at –78 ºC for 0.5 h, the reaction mixture was stirred at room temperature for 3 h. After addition of boron tribromide (0.5 mL, 5.39 mmol) at –78 ºC, the reaction mixture was stirred at room temperature for 1 h. *N*,*N*-Diisopropylethylamine (1.6 mL, 9.11 mmol) was added at 0 ºC and then the reaction mixture was allowed to room temperature. After stirring at 130 ºC for 5 h, the reaction mixture was cooled to room temperature. 5 mL methanol was added to the reaction mixture to quench residual BBr_3. The aqueous layer was separated and extracted with 200 mL dichloromethane. The combined organic layer was condensed in vacuum and purified by column chromatography with a mixture eluent of dichloromethane/petroleum ether (1:9) to obtain a yellow solid (86 mg, yield: 3%). ^{1}H NMR (600 MHz, DMSO-d_6) δ/ppm: 9.138–9.136(d, *J* = 1.22 Hz, 2H), 8.473–8.471(d, *J* = 1.39 Hz, 2H), 8.415–8.401(d, *J* = 8.83 Hz, 2H), 8.348–8.334(d, *J* = 8.14 Hz, 2H), 8.272–8.269(d, *J* = 1.62 Hz, 2H), 8.040–8.012(t, *J* = 8.04 Hz, 1H), 7.670–7.667(d, *J* = 1.80 Hz, 1H), 7.655–7.652(d, *J* = 1.80 Hz, 1H), 1.673 (s, 18H), 1.535 (s, 18H). MALDI-TOF HRMS($C_{46}H_{49}BN_2^+$) m/z. calcd: 640.3983; found: 640.4007.

2. Molecular Structure Characterization Data

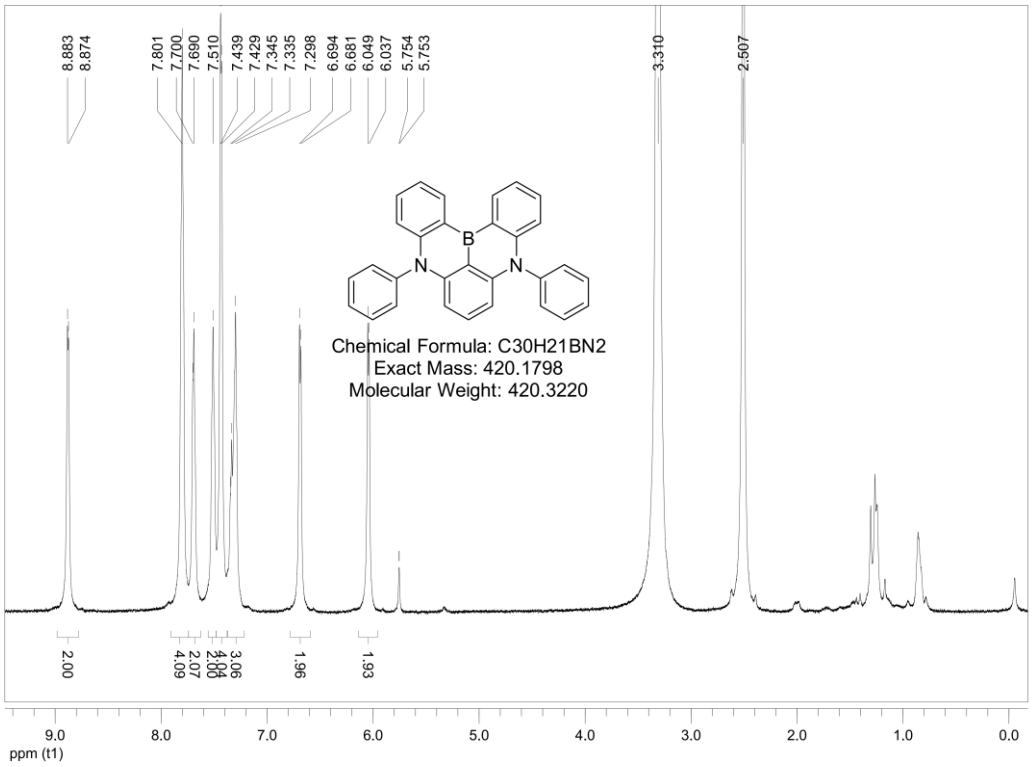

Figure S1. ^{1}H NMR spectrum of **DABNA-1** (600 MHz, DMSO-d_6).

SmartFormula

Formula	Mass	Error	mSigma	DblEq	N rule	Electron Configuration
C 30 H 21 B N 2	420.1792	3.2299	55.6248	22.00	ok	odd

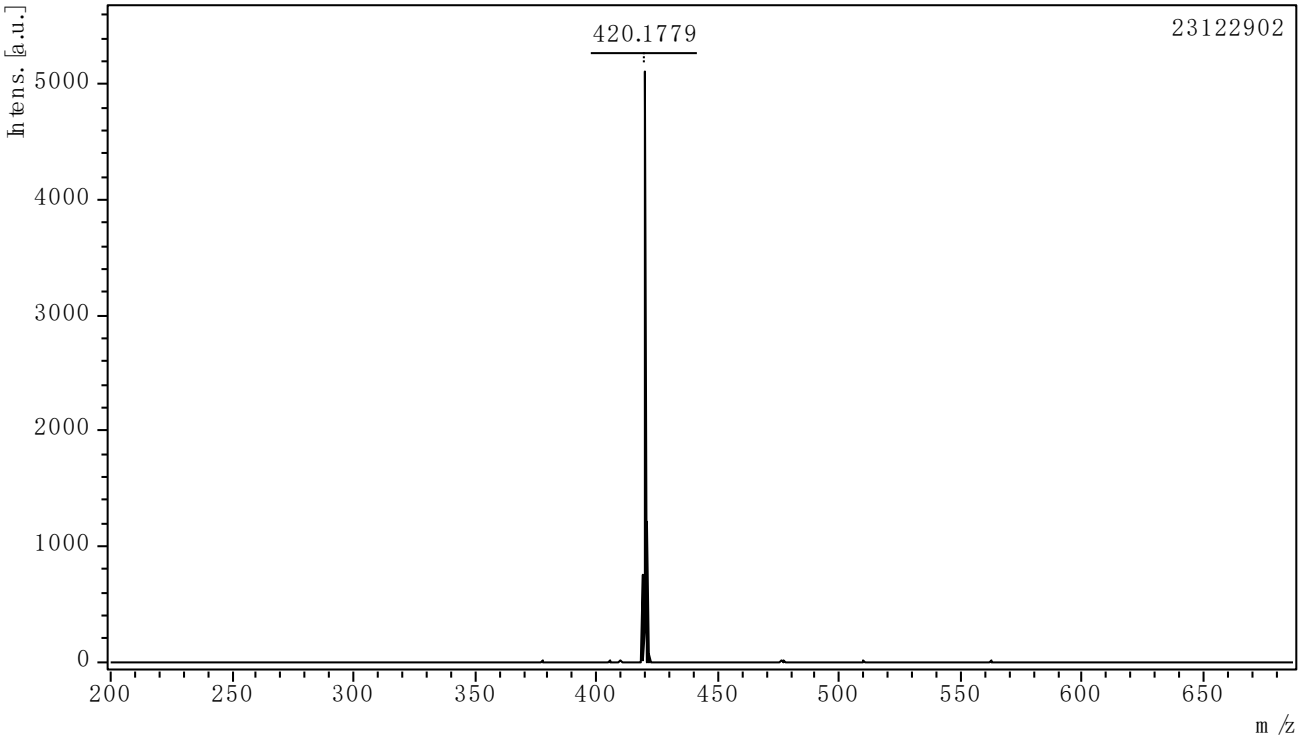

Figure S2. MALDI-TOF HRMS of **DABNA-1**.

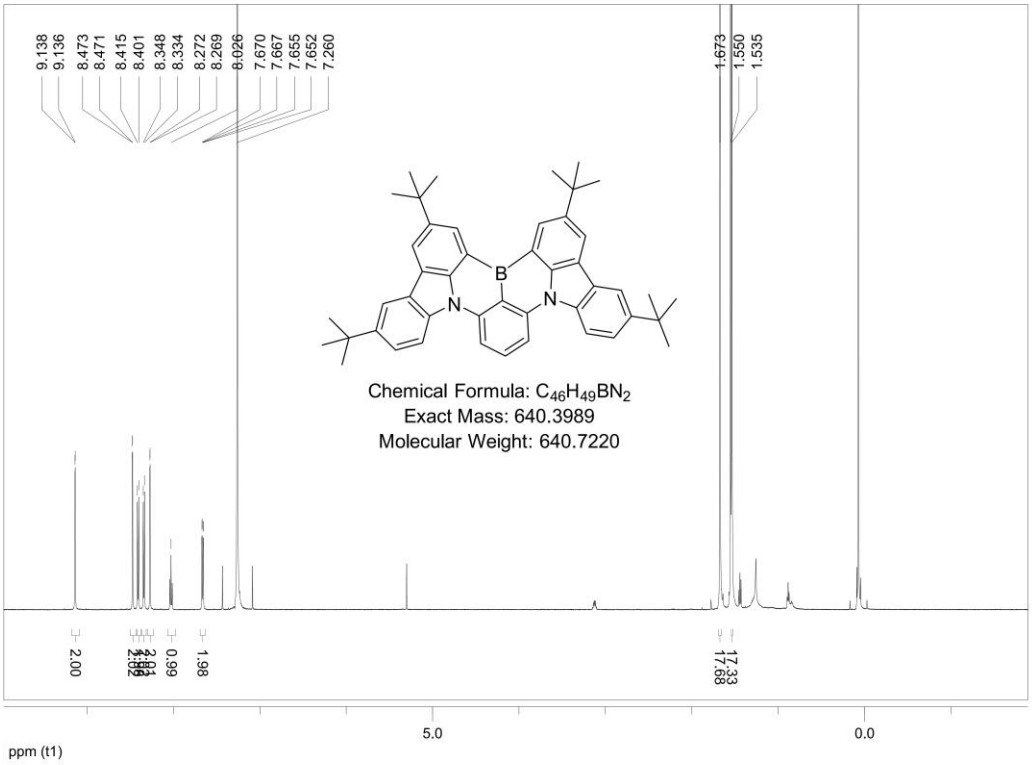

Figure S3. ^{1}H NMR spectrum of **DtBuCzB** (600 MHz, $CDCl_3$).

SmartFormula

Formula	Mass	Error	mSigma	DblEq	N rule	Electron Configuration
C 46 H 49 B N 2	640.3983	3.6242	48.5971	24.00	ok	odd

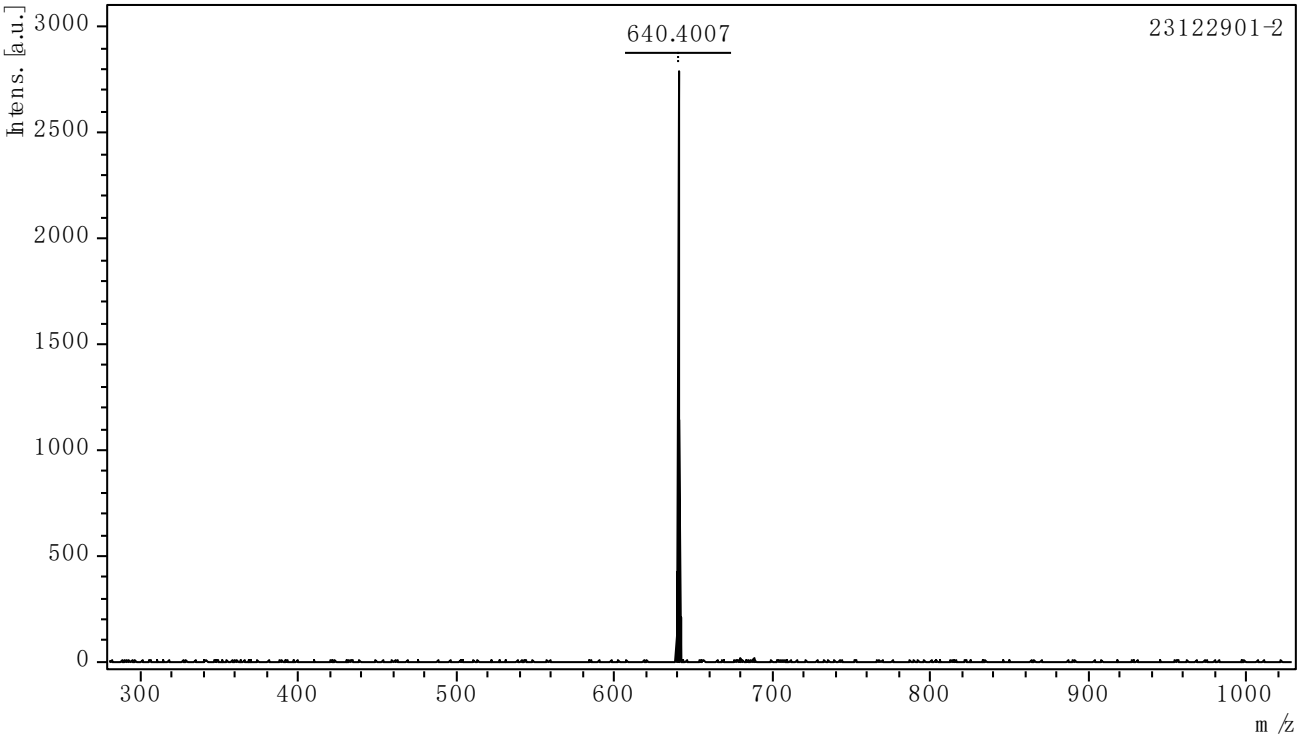

Figure S4. MALDI-TOF HRMS of **DtBuCzB**.

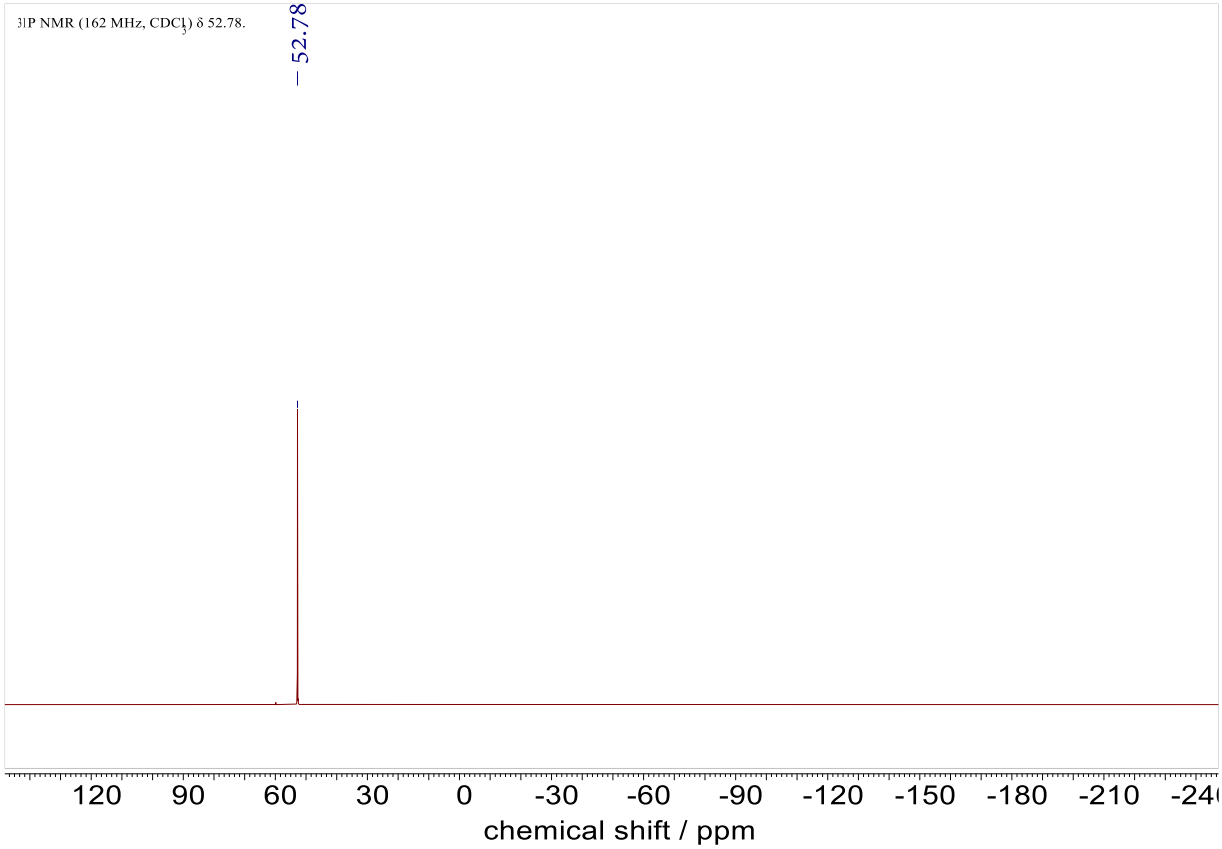

Figure S5. ^{31}P NMR spectrum of **$Et_3P{=}O$** (400 MHz, $CDCl_3$).

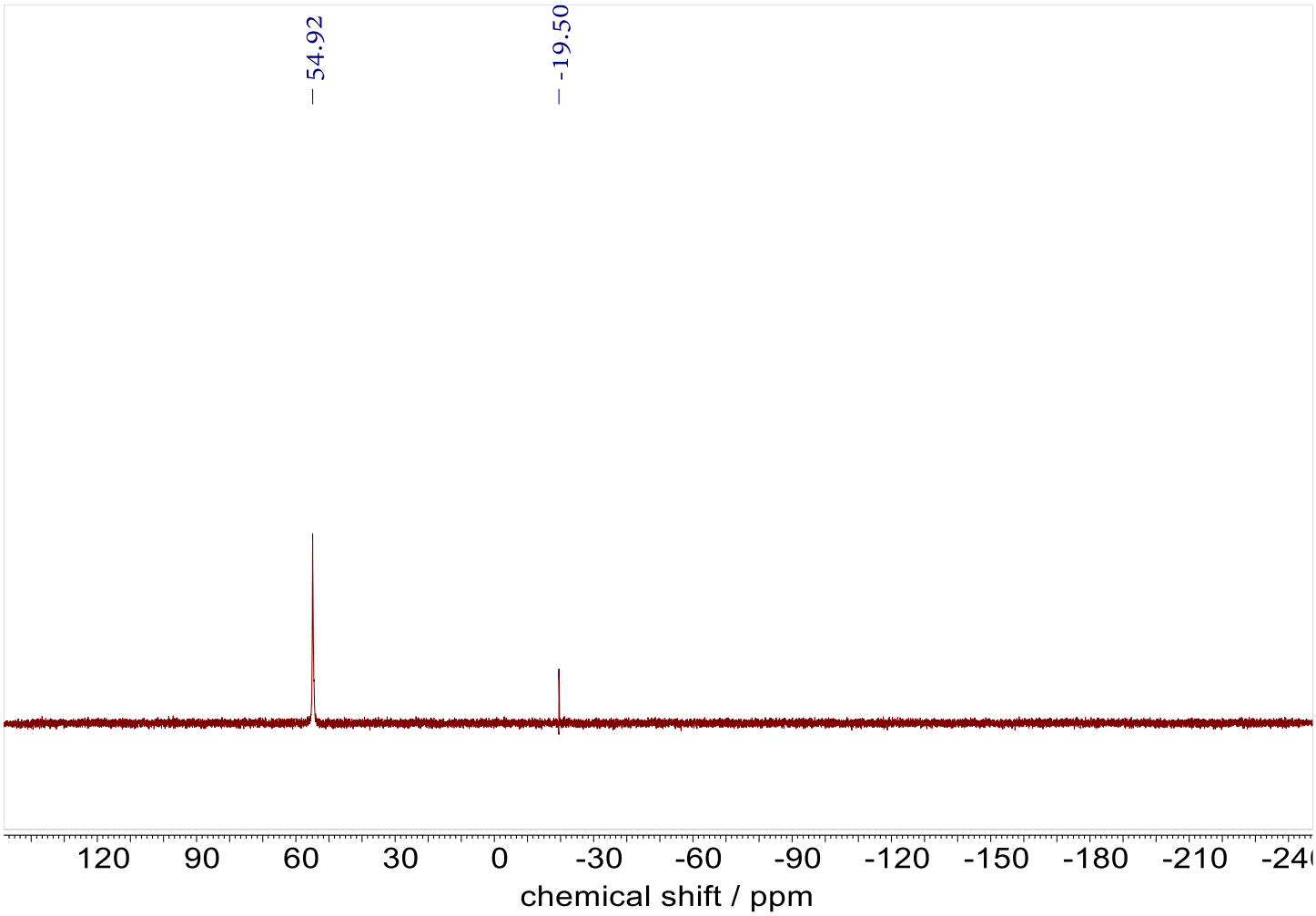

Figure S6. ^{31}P NMR spectrum of **$Et_3P=O$** with **DABNA-1** (400 MHz, $CDCl_3$).

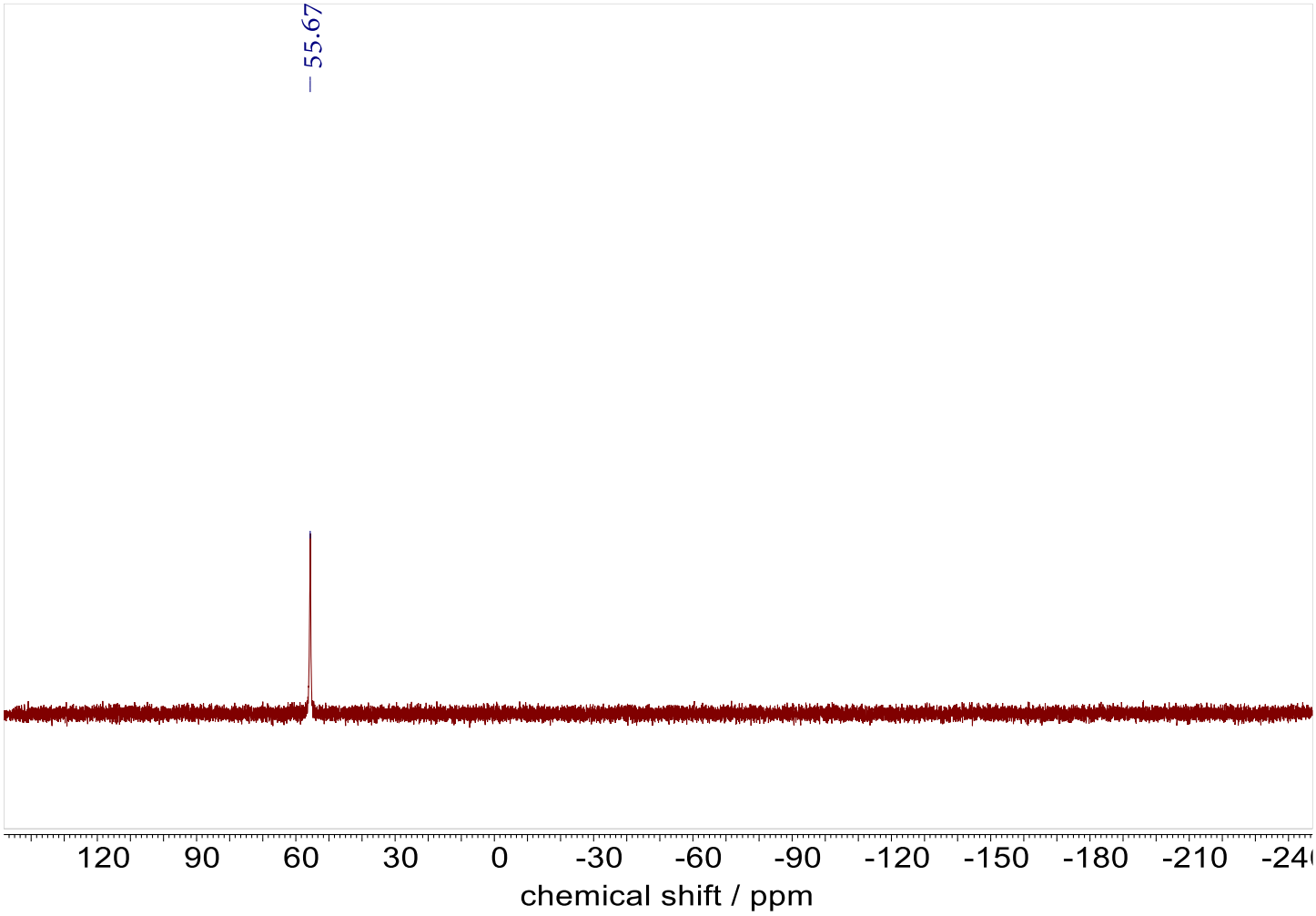

Figure S7. ^{31}P NMR spectrum of **$Et_3P=O$** with **DtBuCzB** (400 MHz, $CDCl_3$).

3. Steady State UV-Vis Absorption Spectra and Fluorescence Emission Spectra.

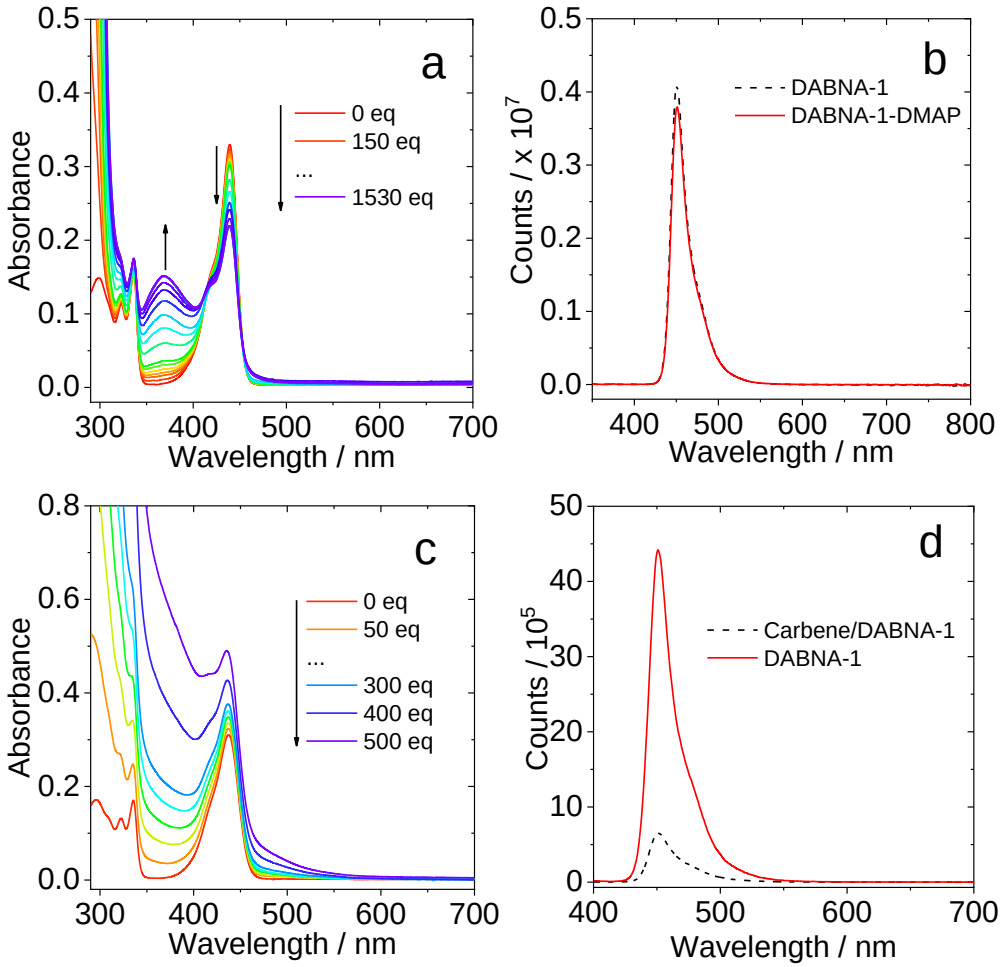

Figure S8. UV-vis absorption spectra of the (a) **DABNA-1** with **DMAP** (1530 eq), (c) **DABNA-1** with **NHC** (500 eq), c = 1.0 × 10^{-5} M. Fluorescence spectra the (b) **DABNA-1-DMAP** (1530 eq), (d) **DABNA-1-NHC** (500 eq) in toluene, optically-matched solutions were used, A = 0.146, λ_{ex} = 336 nm, 20 °C.

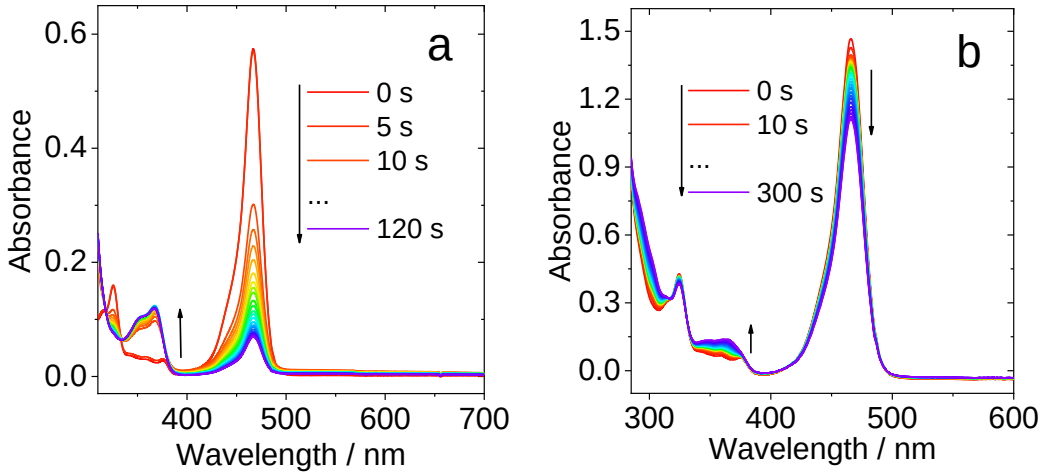

Figure S9. UV-vis absorption spectra of the (a) **DtBuCzB** in toluene with TBAF (4 eq), $c = 1.0 \times 10^{-5}$ M. Spectroelectrochemistry spectra of b) **DtBuCzB** upon potential of –1.45~ –1.48 V(Ag/$AgNO_3$) applied in deaerated DCM containing 0.10 M $Bu_4N[PF_6]$ as supporting electrolyte, Ag/$AgNO_3$ as reference electrode. $c = 2.5 \times 10^{-5}$ M, 20 °C.

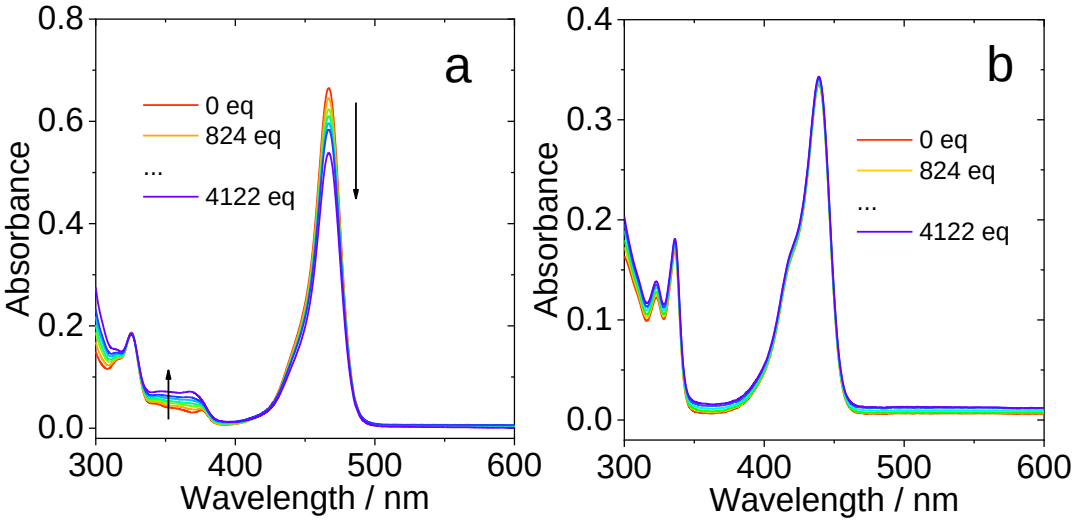

Figure S10. UV-vis absorption spectra of the (a) **DtBuCzB** with pyridine (4122 eq), (b) **DABNA-1** with pyridine (4122 eq), $c = 1.0 \times 10^{-5}$ M.

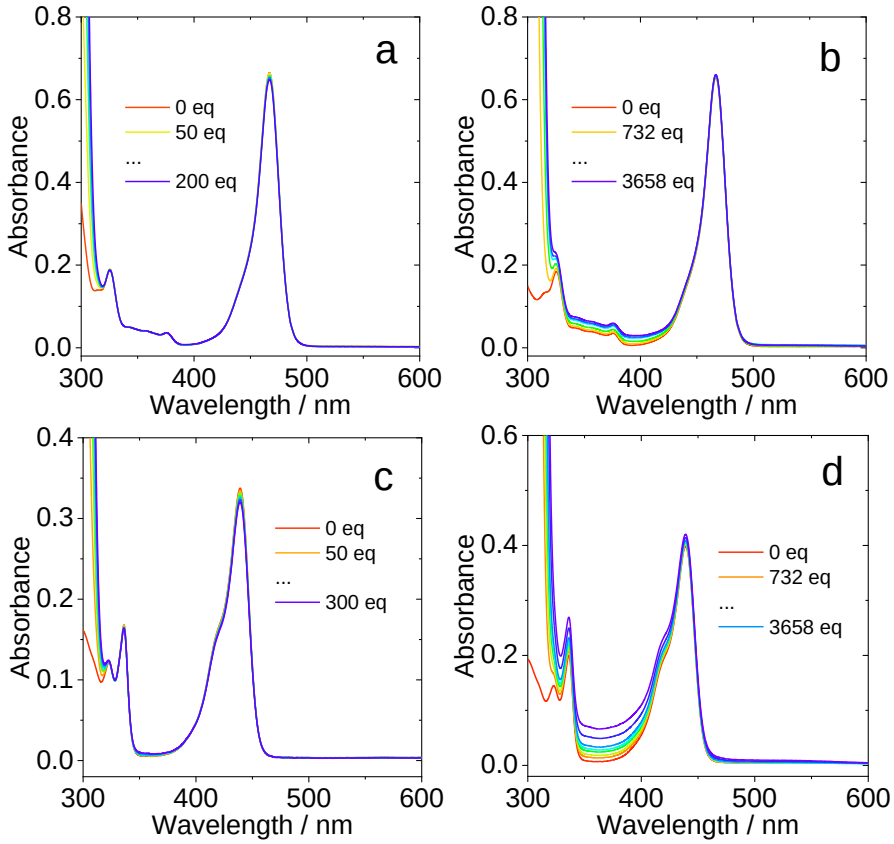

Figure S11. UV-vis absorption spectra of the (a) **DtBuCzB** with Aniline (200 eq), (b) **DtBuCzB** with Aniline (3658 eq), (c) **DABNA-1** with Aniline (200 eq), (d) **DABNA-1** with Aniline (3658 eq), c = 1.0 × 10^{-5} M.

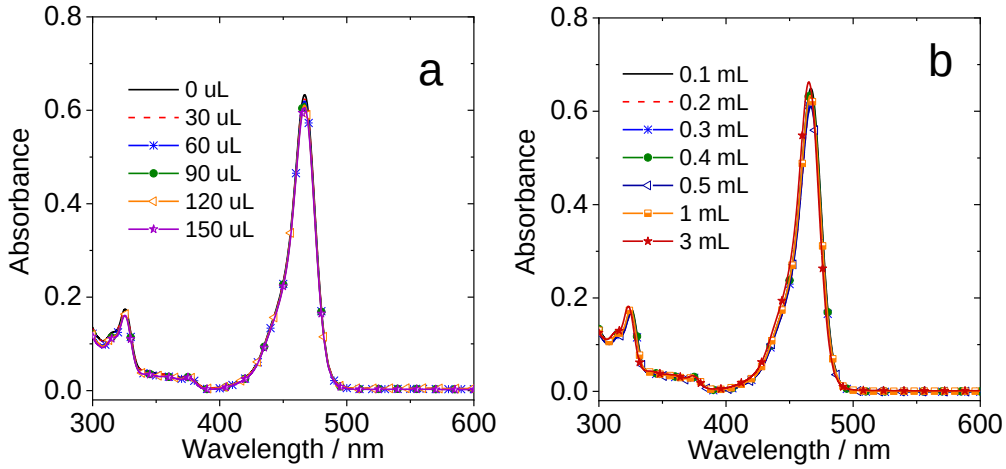

Figure S12. UV-vis absorption spectra of the **DtBuCzB** in toluene with different volumes of 2-MeTHF, c = 1.0 × 10^{-5} M. 20 °C. The total volume of solvent is 3 mL.

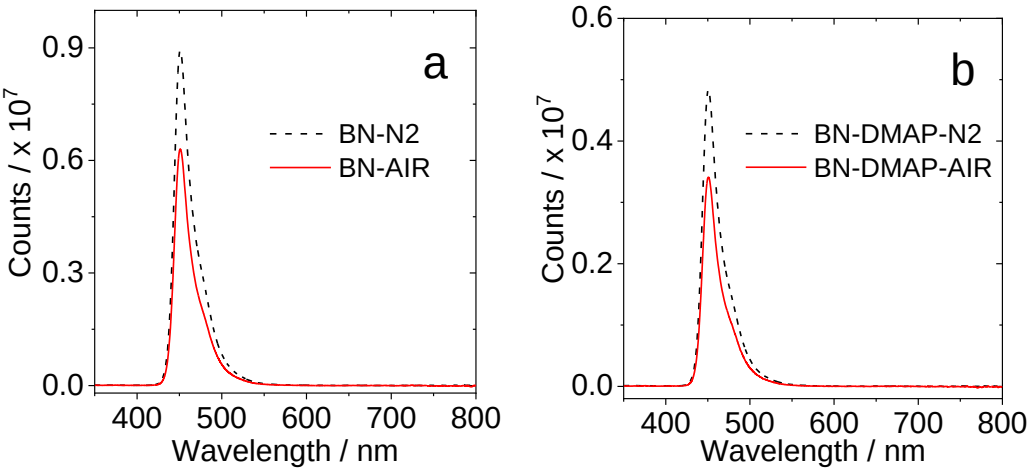

Figure S13. Fluorescence spectra the (a) **DABNA-1** and (b) **DABNA-1-DMAP** in toluene at different atmosphere, optically-matched solutions were used, A = 0.146, λ_{ex} = 336 nm.

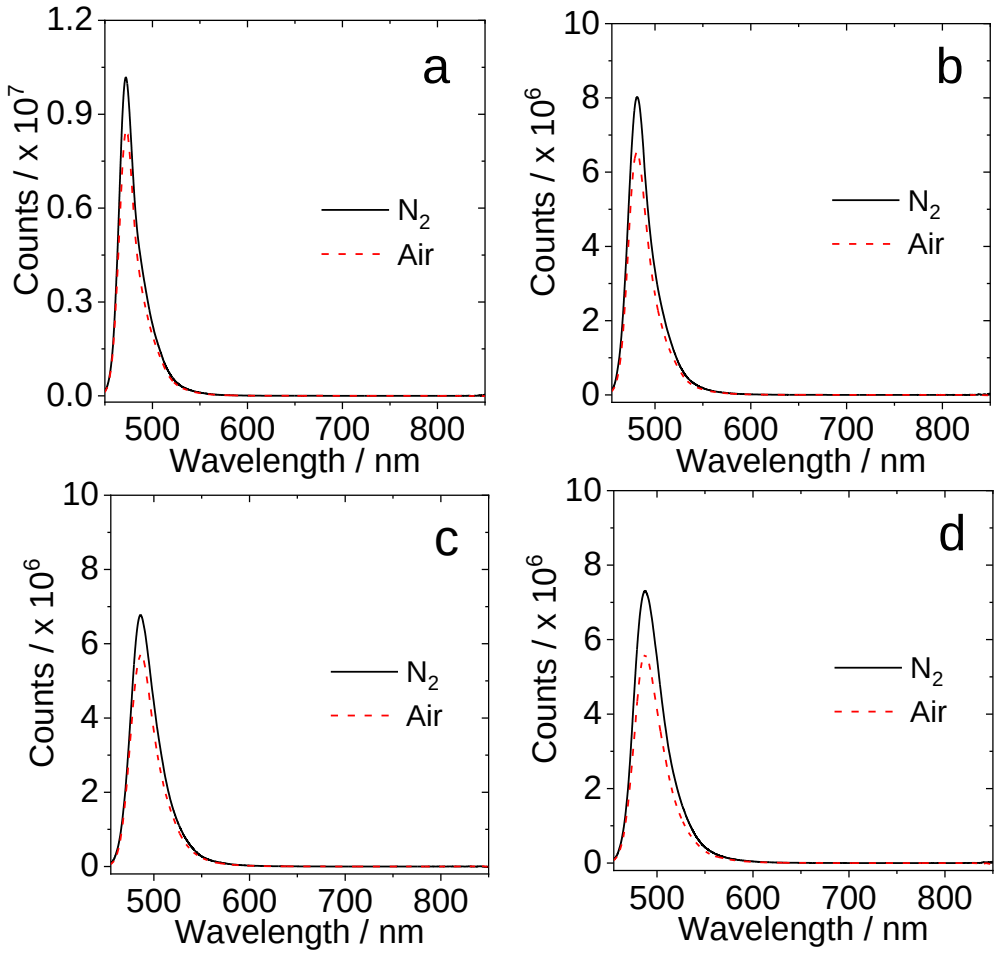

Figure S14. Fluorescence spectra the **DtBuCzB** in (a) cyclohexane, (b) toluene, (c) dichloromethane, (d) acetonitrile, optically-matched solutions were used, A = 0.146, λ_{ex} = 415 nm.

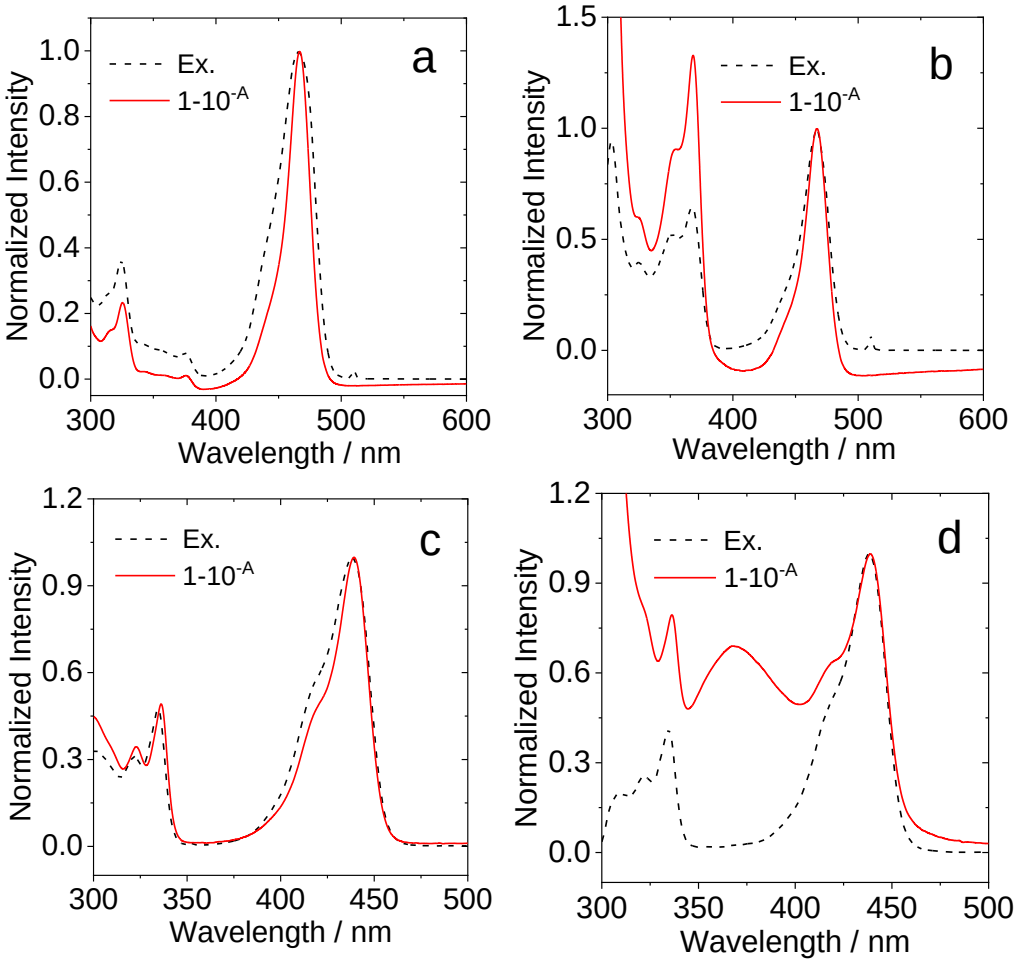

Figure S15. Normalized fluorescence excitation spectra and UV−vis absorption spectra of (a) **DtBuCzB**, (b) **DtBuCzB-DMAP** (50 eq), (c) **DABNA-1** and (d) **DABNA-1-DMAP** (1530 eq) in a toluene, λ_{em} = 510 nm, c = 1.0 × 10^{-5} M, 20 °C.

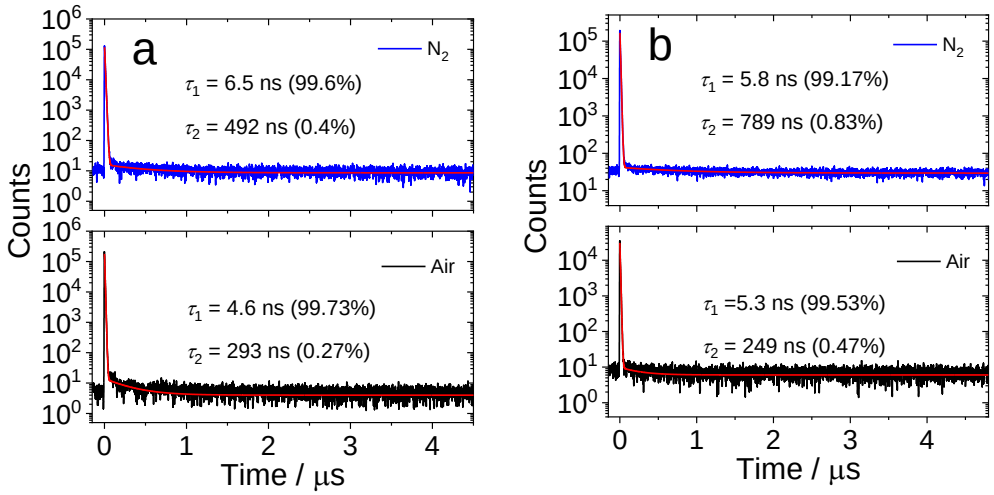

Figure S16. Fluorescence decay traces at 487 nm of **DtBuCzB** with long time range in (a) hexane, (b) dichloromethane under different atmosphere. Excited with picoseconds pulsed laser (λ_{ex} = 340 nm), c = 1.0 × 10^{-5} M, 20 °C.

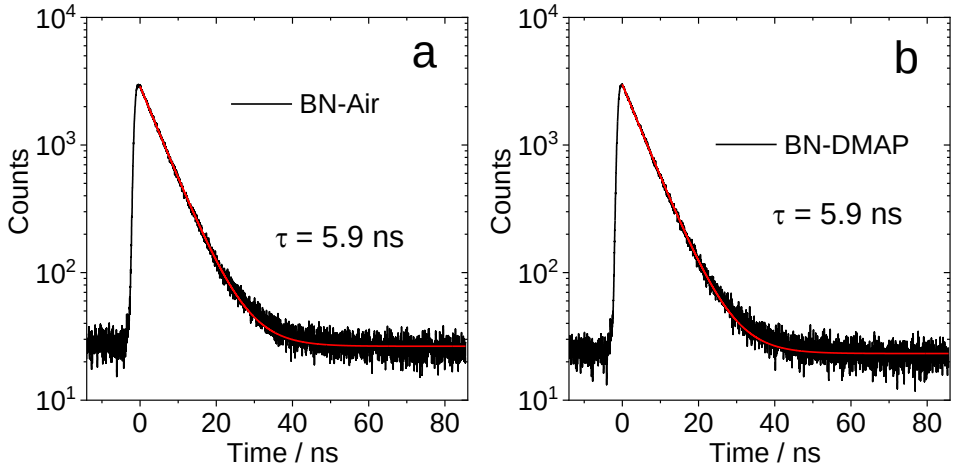

Figure S17. Fluorescence decay traces at 453 nm of **DABNA-1** and at 452 nm of **DABNA-1-DMAP** in toluene under air, λ_{ex} = 340 nm, 20 °C.

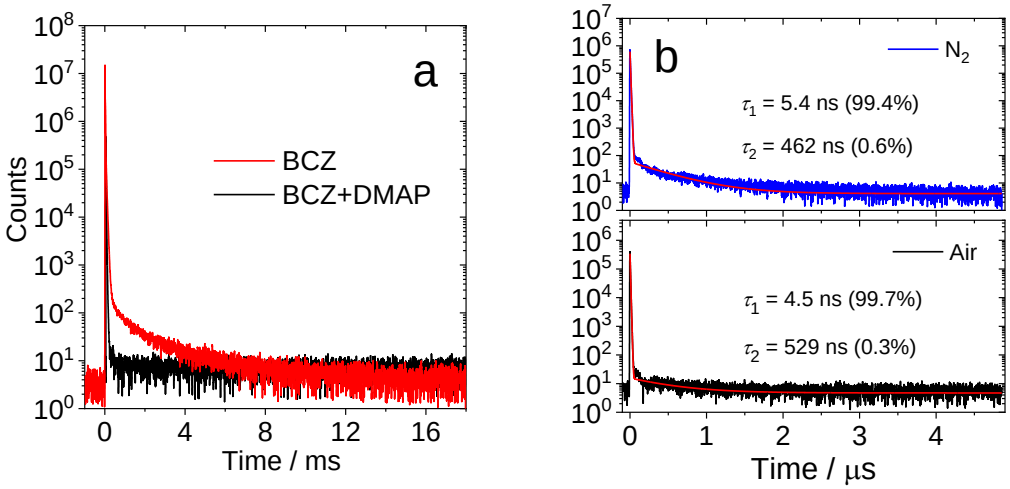

Figure S18. Fluorescence decay traces at 481 nm of (a) **DtBuCzB**, **DtBuCzB** with **DMAP** (50 eq) under N_2 atmosphere, (b) **DtBuCzB** with **DMAP** (50 eq) under different atmospheres (N_2, air). In toluene, λ_{ex} = 340 nm, 20 °C.

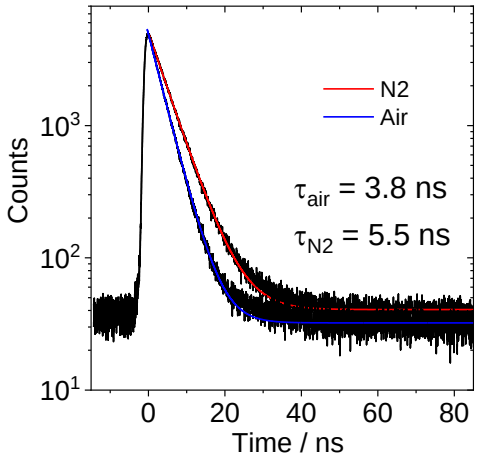

Figure S19. Fluorescence spectra of the **DtBuCzB** in toluene with TBAF (20 eq) under different atmospheres (N_2, air), λ_{ex} = 340 nm, 20 °C.

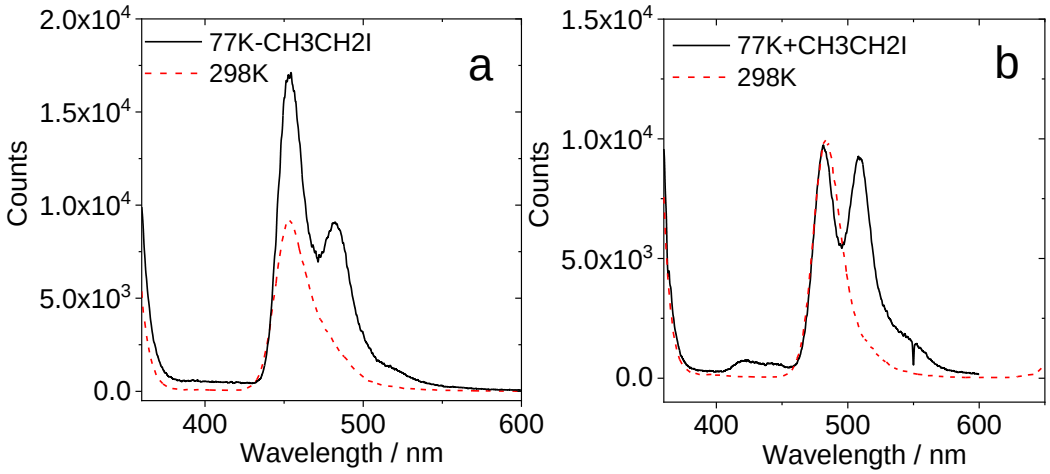

Figure S20. Phosphorescence spectra the (a) **DABNA-1**, (b) **DtBuCzB** in aerated 2-methyltetrahydrofuran or 2-methyltetrahydrofuran/iodoethane (2:1, v/v) at 77 K and 298 K. Excited with picoseconds pulsed laser (λ_{ex} = 340 nm), $c = 1.0 \times 10^{-4}$ M.

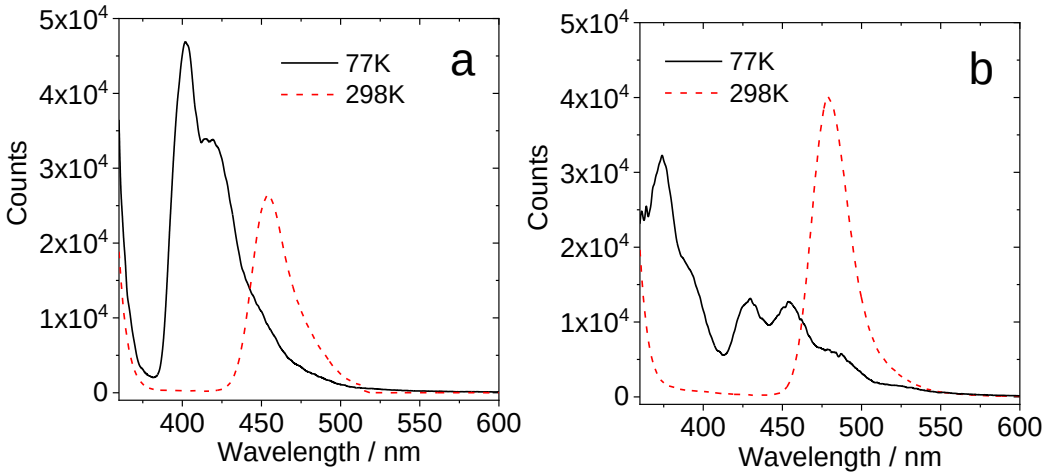

Figure S21. Phosphorescence spectra the (a) **DABNA-1** with **DMAP** (350 eq), (b) **DtBuCzB** with **DMAP** (150 eq) in 2-methyltetrahydrofuran/iodoethane (2:1, v/v) at 77 K and 298 K. Excited with picoseconds pulsed laser (λ_{ex} = 340 nm), c = 1.0 × 10^{-4} M.

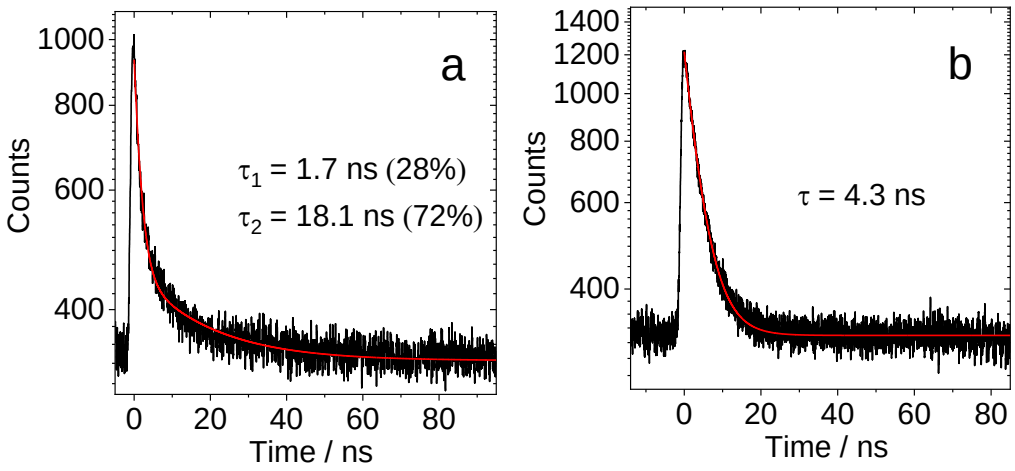

Figure S22. Decay trace of the phosphorescence (a) **DABNA-1** with **DMAP** (350 eq), (b) **DtBuCzB** with **DMAP** (150 eq) at 77 K, λ_{ex} = 340 nm.

4. Transient Absorption Spectra

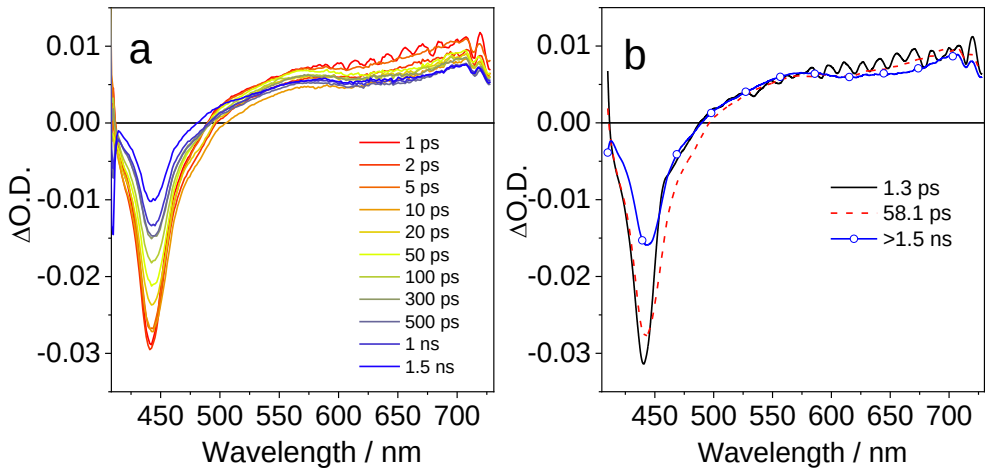

Figure S23. (a) Transient absorption spectra of the **DABNA-1-DMAP** (50 eq) adduct recorded in toluene upon excitation at 400 nm. Panel (b) reports the EADS obtained from global analysis of the transient absorption data.

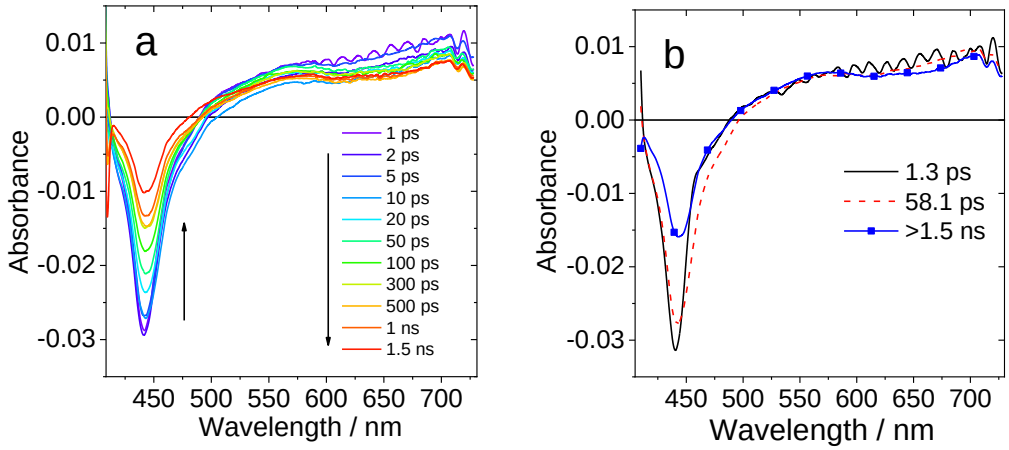

Figure S24. (a) Transient absorption spectra of the **DNBNA-1**: **DMAP** (50 eq) adduct recorded in toluene upon excitation at 400 nm. (b) the EADS obtained from global analysis of the transient absorption data.

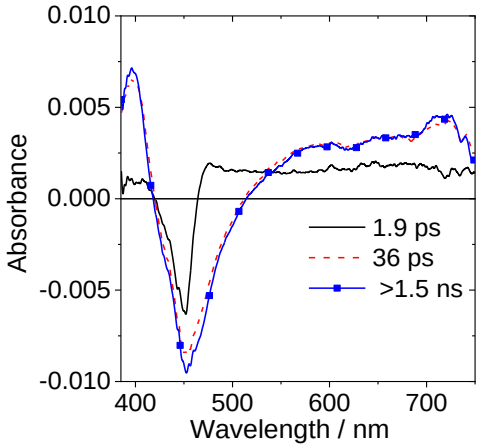

Figure S25. EADS obtained from global analysis of the transient absorption data of the mixture of **DNBNA-1** with 800 equivalents of **DMAP**, upon excitation at 330 nm.

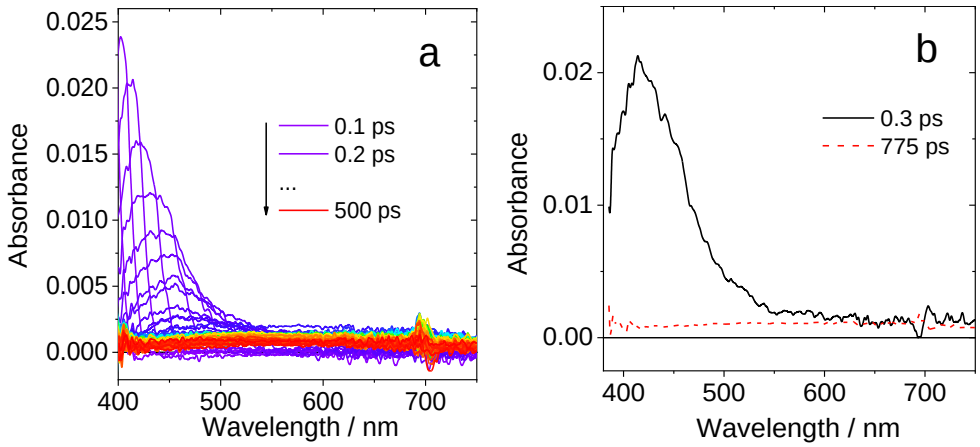

Figure S26. (a) Transient absorption spectra of the **DtBuCzB/NHC** (50 eq) adduct recorded in toluene upon excitation at 350 nm. (b) the EADS obtained from global analysis of the transient absorption data.

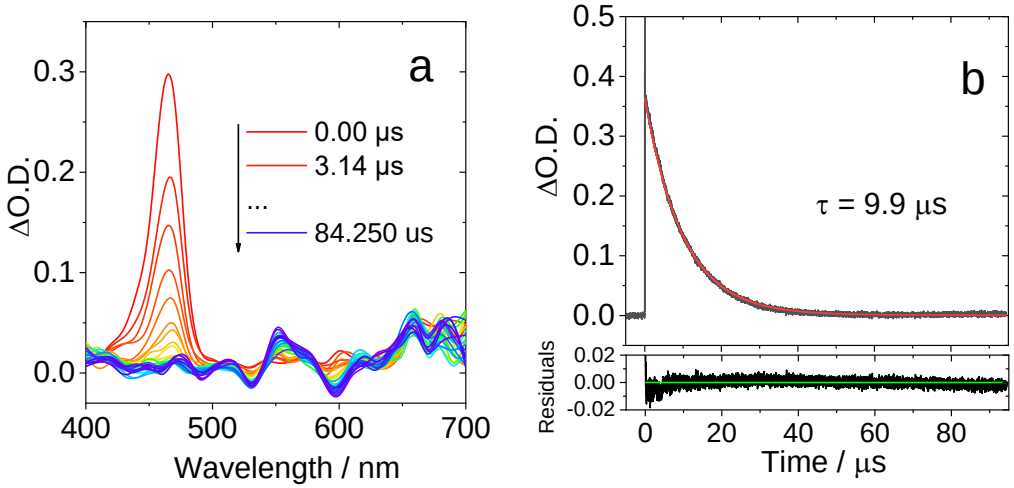

Figure S27. Nanosecond transient absorption spectra of (a) **DtBuCzB** with **DMAP** (50 eq). Decay traces at 465 nm of (b) **DtBuCzB** with **DMAP** (50 eq) in toluene in air, c = 2.0 × 10^{-5} M, λ_{ex} = 355 nm 20 °C.

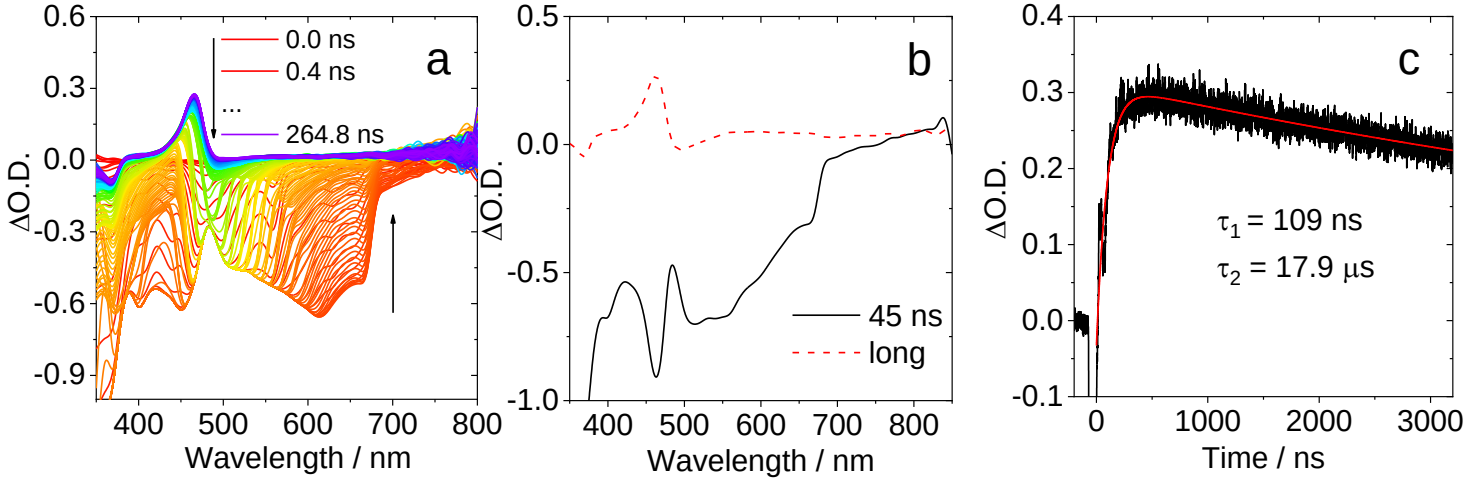

Figure S28. (a) Nanosecond transient absorption spectra of **DtBuCzB** with **DMAP** (50 eq) in toluene/silicone oil, v/v (7:3) in short time range; (b) SADS of **DtBuCzB** with **DMAP**, (c) Decay traces at 470 nm in short time range. c = 2.0 × 10^{-5} M, 20 °C, λ_{ex} = 355 nm.

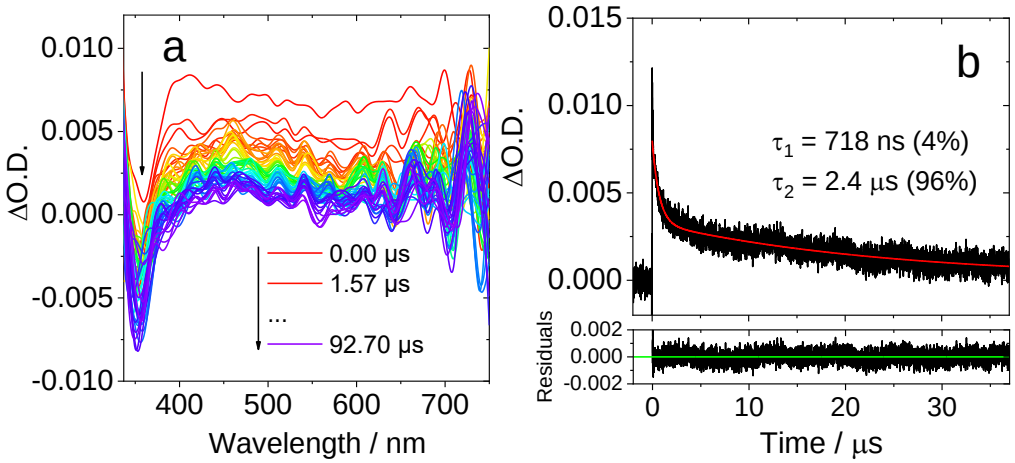

Figure S29. Nanosecond transient absorption spectra of (a) **DtBuCzB** with **NHC** (40 eq); Decay traces at 400 nm of (d) **DtBuCzB** with **NHC** (40 eq) in acetonitrile, *c* [**DtBuCzB**] = 2.0 × 10^{-5} M, 20 °C.

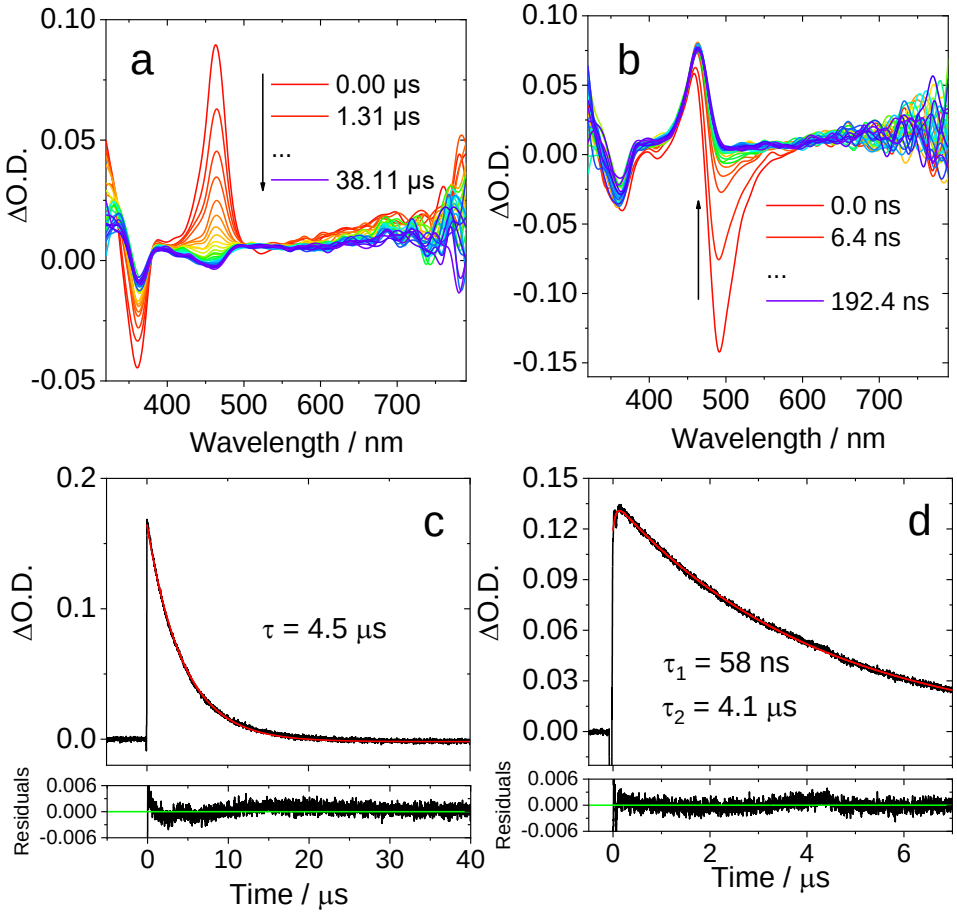

Figure S30. Nanosecond transient absorption spectra of **DtBuCzB** with **DMAP** (50 eq) (a) in long timerange; (b) in short timerange; Decay traces at 470 nm of (d) **DtBuCzB** with **DMAP** (50 eq) in acetonitrile, *c* [**DtBuCzB**] = 2.0 × 10^{-5} M, 20 °C

Table S1. Lifetime of DtBuCzB with DMAP in toluene/silicone oil at 470 nm [a]

Lifetime at 470 nm	Toluene/silicone oil, v/v		
	9:1	**8:2**	**7:3**
DtBuCzB with 10 eq **DMAP**	28.0 μs	18.0 μs	_ [b]
DtBuCzB with 50 eq **DMAP**	10.9 μs	9.5 μs	8.9 μs
DtBuCzB with 150 eq **DMAP**	5.2 μs	_ [b]	_ [b]

[a] $c = 2.0 \times 10^{-5}$ M, 20 °C, $\lambda_{ex} = 355$ nm. [b] Not detected.

By increasing the viscosity of the solvent, the apparent lifetime of the photoenerated **DtBuCzB** in the presence of 50 eq **DMAP** was decreased. Moreover, the lifetimes of different **DMAP** equivalents were studied and it became progressively shorter as the **DMAP** concentration increased.

5. Electrochemical Studies: Cyclic Voltammograms

Table S2. Electrochemical Redox Potentials of the Compounds [a]

Compounds	E_{Ox} (V)	E_{Red} (V)
DtBuCzB	+0.65	–2.13
DABNA-1	+0.70	–1.83

[a] Cyclic voltammetry in deaerated ACN containing a 0.10 M Bu_4NPF_6. Pt electrode is counter electrode, glassy carbon electrode is working electrode, and $Ag/AgNO_3$ couple as the reference electrode. [b] E_{00} = 2.61 eV. [c] E_{00} = 2.77 eV. E_{00} (E_{00} = 1240/λ) is the singlet state energy of compounds, λ is the wavelength of the crossing point of normalized UV–vis absorption spectra and fluorescence emission spectra.

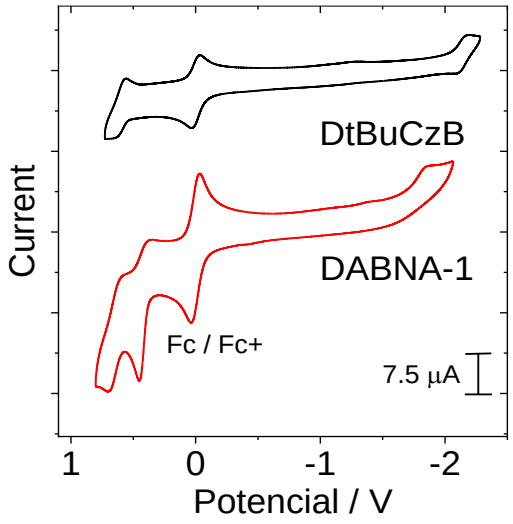

Figure S31. Cyclic voltammograms of the compounds in deaerated ACN. Ferrocene (Fc/Fc+) was used as the internal reference (set as 0 V in the cyclic voltammograms). Conditions: in deaerated solvents containing 0.10 M $Bu_4N[PF_6]$ as the supporting electrolyte, and $Ag/AgNO_3$ as the reference electrode. Scan rate: 100 mV s^{-1} and c = 1.0 × 10^{-4} M.

6. Theoretical Computations.

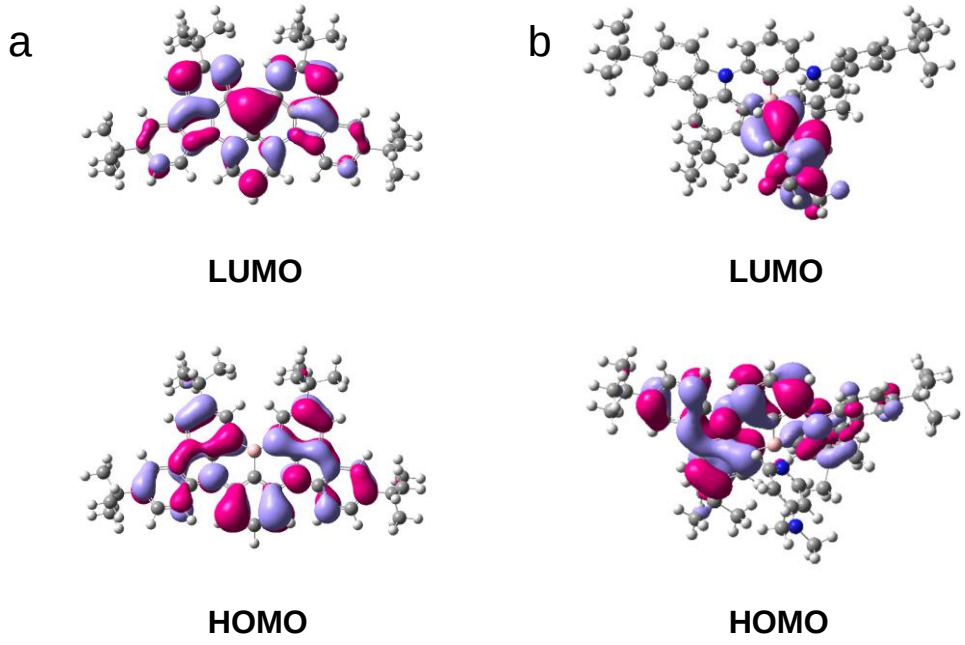

Figure S32. HOMO/LUMO energy levels of (a) **DtBuCzB** and (b) **DtBuCzB-DMAP** at ground state geometry, isovalues: 0.02. Calculations were performed at the (B3LYP/6-31G) level with Gaussian 16.

The distance between **DtBuCzB** and **DMAP** is 1.72 Å by optimised ground state configuration.

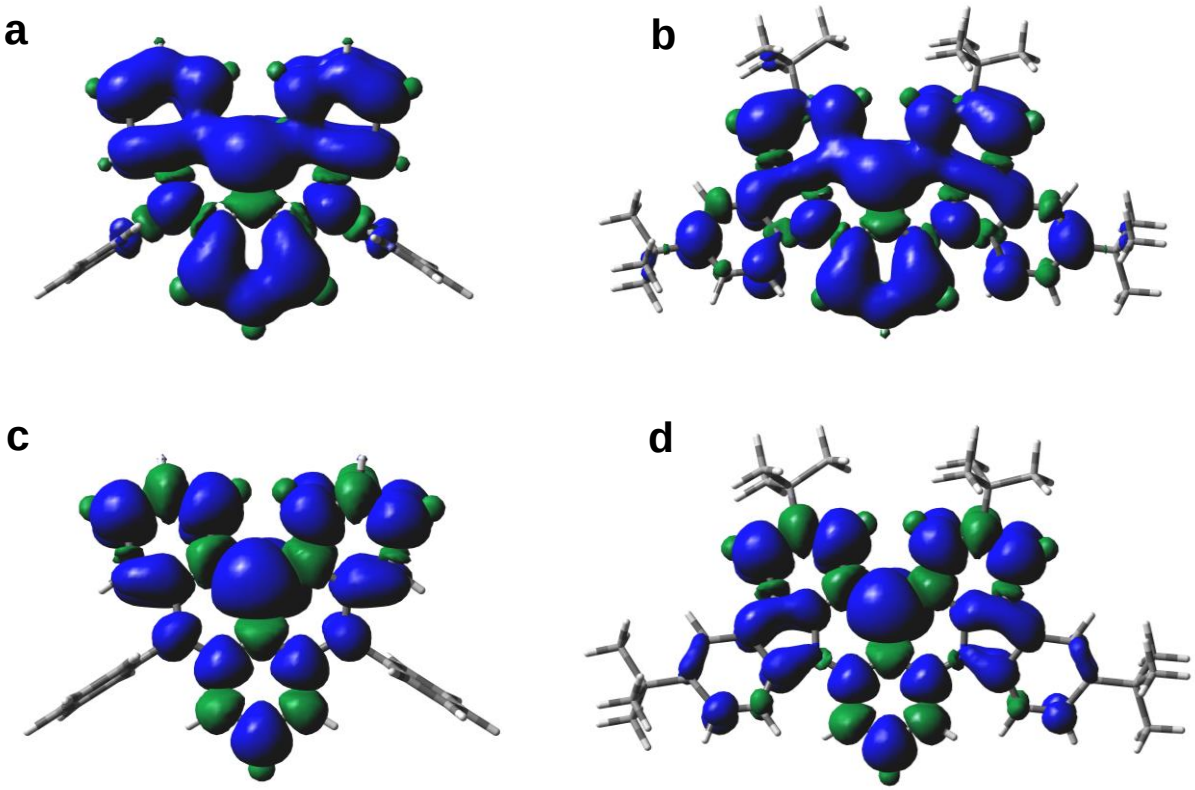

Figure S33. Spin density distribution of (a) **DABNA-1** triplet state, (b) **DtBuCzB** triplet state, (c) **DABNA-1** anion, (d) **DtBuCzB** anion, isovalues: 0.0004. Dichloromethane was used in the calculations. Calculations were performed at the (B3LYP/6-31G) level with Gaussian 16.

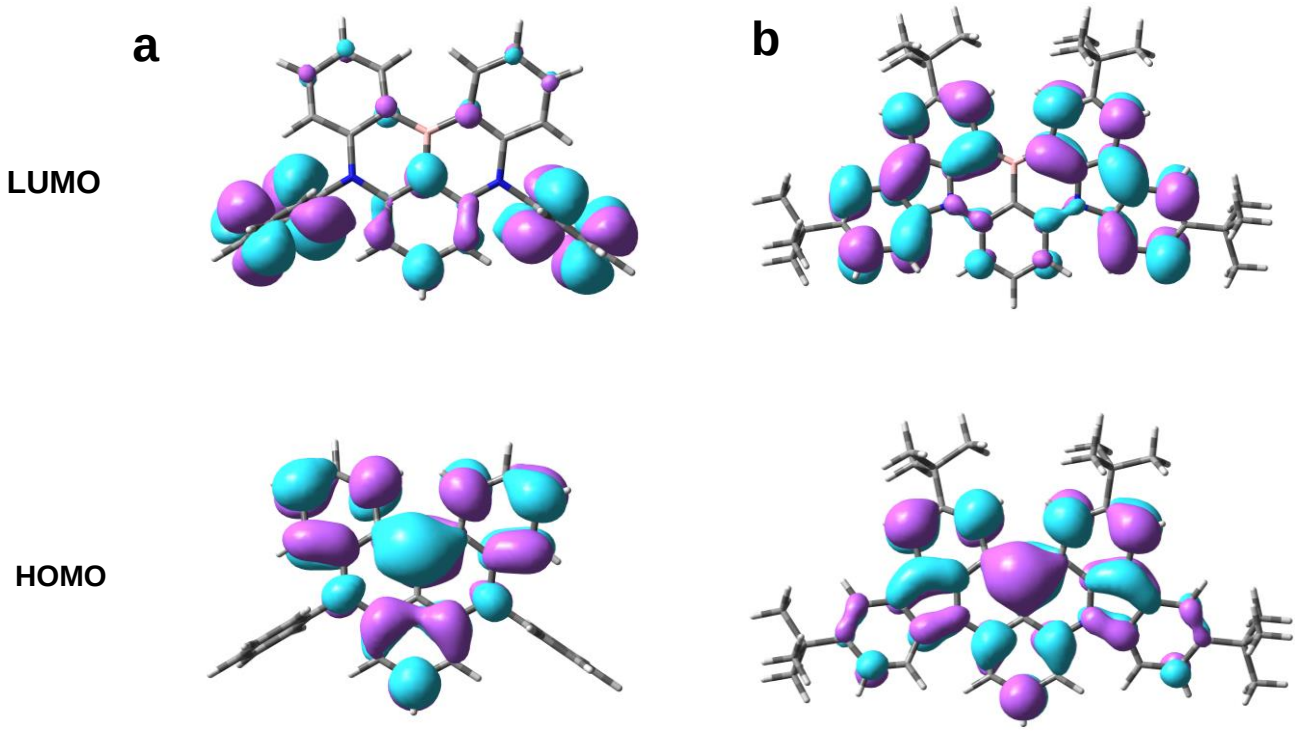

Figure S34. Molecular orbital of $D_0 \rightarrow D_1$ absorption for (a) **DABNA-1** anion, (b) **DtBuCzB** anion, isovalues: 0.0004. Dichloromethane was used in the calculations. Calculations were performed at the (B3LYP/6-31G) level with Gaussian 16.

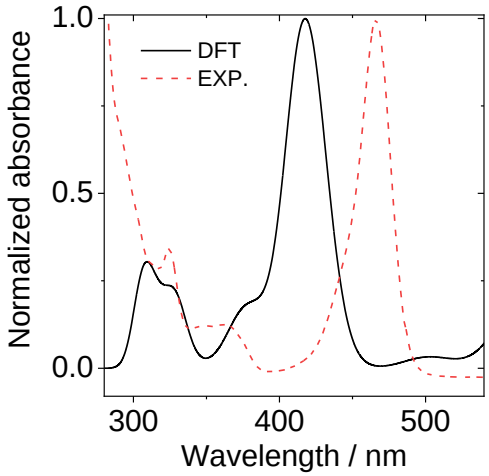

Figure S35. UV-vis absorption spectra of the **DtBuCzB** anion by DFT and Spectroelectrochemistry experiment. Calculations were performed at the (B3LYP/6-31G) level with Gaussian 16.

Reference

(1) Hatakeyama, T.; Shiren, K.; Nakajima, K.; Nomura, S.; Nakatsuka, S.; Kinoshita, K.; Ni, J.; Ono, Y.; Ikuta, T., Ultrapure Blue Thermally Activated Delayed Fluorescence Molecules: Efficient HOMO–LUMO Separation by the Multiple Resonance Effect. *Adv. Mater.* **2016**, *28* (14), 2777–2781.

(2) Zhang, Y.; Zhang, D.; Wei, J.; Liu, Z.; Lu, Y.; Duan, L., Multi-Resonance Induced Thermally Activated Delayed Fluorophores for Narrowband Green OLEDs. *Angew. Chem., Int. Ed.* **2019**, *58* (47), 16912–16917.

(3) Snellenburg, J. J.; Laptenok, S.; Seger, R.; Mullen, K. M.; van Stokkum, I. H. M., Glotaran: A Java-Based Graphical User Interface for the R Package TIMP. *J. Stat. Softw.* **2012**, *49* (3), 1 - 22.

(4) Stoll, S.; Schweiger, A., EasySpin, a Comprehensive Software Package for Spectral Simulation and Analysis in EPR. *J. Magn. Reson.* **2006**, *178* (1), 42–55.

(5) Frisch, M. J.; Trucks, G. W.; Schlegel, H. B.; Scuseria, G. E.; Robb, M. A.; Cheeseman, J. R.; Scalmani, G.; Barone, V.; Petersson, G. A.; Nakatsuji, H.; Li, X.; Caricato, M.; Marenich, A. V.; Bloino, J.; Janesko, B. G.; Gomperts, R.; Mennucci, B.; Hratchian, H. P.; Ortiz, J. V.; Izmaylov, A. F.; Sonnenberg, J. L.; Williams; Ding, F.; Lipparini, F.; Egidi, F.; Goings, J.; Peng, B.; Petrone, A.; Henderson, T.; Ranasinghe, D.; Zakrzewski, V. G.; Gao, J.; Rega, N.; Zheng, G.; Liang, W.; Hada, M.; Ehara, M.; Toyota, K.; Fukuda, R.; Hasegawa, J.; Ishida, M.; Nakajima, T.; Honda, Y.; Kitao, O.; Nakai, H.; Vreven, T.; Throssell, K.; Montgomery Jr., J. A.; Peralta, J. E.; Ogliaro, F.; Bearpark, M. J.; Heyd, J. J.; Brothers, E. N.; Kudin, K. N.; Staroverov, V. N.; Keith, T. A.; Kobayashi, R.; Normand, J.; Raghavachari, K.; Rendell, A. P.; Burant, J. C.; Iyengar, S. S.; Tomasi, J.; Cossi, M.; Millam, J. M.; Klene, M.; Adamo, C.; Cammi, R.; Ochterski, J. W.; Martin, R. L.; Morokuma, K.; Farkas, O.; Foresman, J. B.; Fox, D. J. *Gaussian 16 Rev. C.01*, Wallingford, CT, 2016.

(6) Neese, F.; Wennmohs, F.; Becker, U.; Riplinger, C., The ORCA Quantum Chemistry Program Package. *J. Chem. Phys.* **2020**, *152*, 224108.

(7) Neese, F., Software update: The ORCA program system—Version 5.0. *WIRES Comput. Mol. Sci.* **2022**, *12*, e1606.